# NACA

# RESEARCH MEMORANDUM

INVESTIGATION OF A SHROUDED AND AN UNSHROUDED

AXIAL-FLOW SUPERSONIC COMPRESSOR

By Emanuel Boxer and John R. Erwin

Langley Aeronautical Laboratory Langley Air Force Base, Va.

# NATIONAL ADVISORY COMMITTEE FOR AERONAUTICS

WASHINGTON

September 15, 1950 Declassified April 13, 1953

# NATIONAL ADVISORY COMMITTEE FOR AERONAUTICS

# RESEARCH MEMORANDUM

# INVESTIGATION OF A SHROUDED AND AN UNSHROUDED

AXIAL-FLOW SUPERSONIC COMPRESSOR

By Emanuel Boxer and John R. Erwin

#### SUMMARY

An unshrouded axial-flow supersonic compressor rotor has been designed based upon the experience gained through tests of the original shrouded rotor. A study of two-dimensional blade sections led to the attainment of thicker blades which alleviated the necessity of a shroud attached to the blade tips. A 16-inch-tip-diameter rotor was constructed and an investigation was made in Freon-12 gas at the NACA Langley Laboratory through a range of equivalent tip speeds from 866 to 1680 feet per second when converted to standard sea-level air. As designed, the unshrouded rotor produced a pressure ratio across the rotor of 2.03 with an efficiency of 83.5 percent at a weight flow of 28.0 pounds per second. Operating without inlet guide vanes, the rotor produced a pressure ratio of 2.20 at an efficiency of 84.5 percent and a flow rate of 27.8 pounds per second. Reasonable agreement was obtained between test results and design values of the relative total pressure and Mach number at the exit of the blades.

Tests results for an accurately fabricated model of the original shrouded rotor are presented for direct comparison with data obtained with the use of a similar rotor tested in air at the NACA Lewis Flight Propulsion Laboratory. At the design tip speed of 1610 feet per second, the shrouded rotor tested in Freon produced a total pressure ratio of 1.98 with 84-percent efficiency at a weight flow of 27.6 pounds per second of air, as compared with 1.93, 79 percent, and 25.8 pounds per second for the similar rotor in air. The differences are attributed to the fact that the flow into the blading was not entirely supersonic for the tests in air.

### INTRODUCTION

Previous investigations of axial-flow compressor rotors operating with supersonic velocities relative to the blade rows have been concerned mainly with demonstrating the validity of theoretical concepts of the aerodynamic problems involved. The basic principles of supersonic operation of axial-flow compressors presented by Kantrowitz in reference 1 were proven to be correct by experimental results of a rotor tested in Freon-12 gas (reference 2). This rotor, although inaccurately constructed, exhibited the characteristics of supersonic operation, that is, constant equivalent weight flow at design speed invariable with back pressure. The next logical step, to demonstrate the performance in air, was undertaken with the use of a similar rotor at the NACA Lewis Flight Propulsion Laboratory and the results are reported in references 3 and 4. The results of tests made in Freon with the use of the reconstructed rotor mentioned in reference 2 are presented in the present paper for a more accurate comparison of the operation of the supersonic compressor in Freon and in air.

The desirable characteristics of supersonic axial-flow compressors, high-pressure ratio per stage and high mass flow per unit area, were demonstrated with these thin-blade shrouded rotors. For industrial acceptance of the supersonic compressor, a structurally sound design incorporating thicker blade sections to alleviate the need for the blade shroud is desirable. The purpose of this paper is to describe a method by which thicker blade sections were obtained and to describe in detail the design, tests, and performance of an unshrouded rotor operated in Freon-12 gas.

The tests of the unshrouded rotor were begun at the NACA Langley Laboratory on August 28, 1947.

#### SYMBOLS

а	velocity of sound, feet per second
A	area, square feet
$c_p$	specific heat at constant pressure, foot-pounds per slug per ${}^{\mathrm{o}}\mathrm{F}$
g	acceleration due to gravity (32.2 feet per second per second)
M	Mach number, ratio of flow velocity to the velocity of sound $\left(\frac{\nabla}{a}\right)$

n rotational speed of rotor, revolutions per second

P total or stagnation pressure, pounds per square foot

p static pressure, pounds per square foot

R gas constant (for pure Freon 12, 411.5; for air, 1716 foot-pound per slug oF)

r radial position measured from axis, feet

T temperature, oF absolute

ΔT' adiabatic stagnation-temperature rise

$$\frac{\left(\int_{r_{h}}^{r_{t}} \left[T_{o}\left(\frac{P_{5_{s}}}{P_{o}}\right)^{\frac{R_{m}}{c_{p_{m}}}} - T_{o}\right] \rho V_{a} r dr}{\int_{r_{h}}^{r_{t}} \rho V_{a} r dr}\right)$$

ΔT measured stagnation-temperature rise

U rotational velocity (2πnr) at radius r, feet per second

V velocity of fluid, feet per second

 $\overline{\overline{V}}$  average velocity of fluid, feet per second

W weight flow 
$$\left(2\pi g \int_{\mathbf{r}_h}^{\mathbf{r}_t} \rho V_{\mathbf{a}} \mathbf{r} d\mathbf{r}\right)$$

 $\beta$  angle between flow direction and the axis, degrees

 $\delta$  ratio of actual inlet total pressure to standard sea-level pressure (  $P_{0}/2116)$ 

$$\eta_{\text{p}}$$
 adiabatic efficiency evaluated from survey

$$\frac{\int_{r_{h}}^{r_{t}} c_{p} \Delta T' \rho V_{a} r dr}{\int_{r_{h}}^{r_{t}} U_{5} V_{5}_{tan} \rho_{5} V_{a5} r dr - \int_{r_{h}}^{r_{t}} U_{1} V_{1}_{tan} \rho_{1} V_{a_{1}} r dr}$$

$$\eta_t$$
 adiabatic efficiency  $\left(\frac{\Delta T!}{\Delta T}\right)$ 

- γ ratio of specific heats (1.40 for air and 1.125 for pure Freon 12)
- θ ratio of actual inlet stagnation temperature to standard sealevel temperature  $(T_0/518.4)$
- ø turning angle, rotor coordinates, degrees
- ρ density, slugs per cubic foot

# Subscripts:

a axial

av average

h root

m mixture, Freon and air

t tip

tan tangential

s stagnation

o initial stagnation conditions

1 rotor entrance, stationary coordinates

2 rotor entrance, rotor coordinates

- 4 rotor exit, rotor coordinates
- 5 rotor exit, stationary coordinates
  Prime denotes condition after waves.

# DESIGN OF UNSHROUDED ROTOR (ROTOR 2)

Rotor-design requirements. The general design conditions for the unshrouded rotor (also referred to as rotor 2) were the same as for the shrouded rotor reported in reference 2 and are outlined below:

Tip diameter, inches		16
Hub/tip diameter		0.75
Axial Mach number at entrance to rotor		0.80
Tip speed in air at standard conditions, feet per second		1600
Prerotation upstream of rotor	Little or	none
Maximum Mach number into stator		0.80

At the time that the unshrouded rotor was designed, the belief was held that the entrance Mach number to a particular blade section was the sole determinant of the thickness of that section. In order to have the blades tapering in the usual manner from root to tip, this consideration required a greater Mach number relative to the rotor at the root than at the tip. This Mach number distribution was also desired for a second consideration of this rotor design since lowering the entrance Mach number at the tip, and hence the pressure rise across the normal shock in conjunction with reduced turning angle were expected to reduce the separation observed near the tip of the shrouded supersonic rotor.

A further condition held to be desirable was the existence of constant total pressures relative to the stator. Theoretical evaluation of frictionless mixing loss due to nonuniform total pressures in straight pipes by using the method of reference 5 indicates that a loss of 2 percent in total pressure occurs for a 20-percent variation of total pressure at a Mach number of 0.8. As the stator-entrance Mach number will be of the order of 0.8, it is evident that nonuniform total pressure would produce significant losses. The condition of constant exit total pressure can be produced more readily if the rotor-entrance Mach number decreases from root to tip. This will give a more nearly constant entrance total pressure than if the design were for a constant or outwardly increasing value of M2. With the Mach number distributions used, it is easier to equalize the power input and the exit total pressures at the various diameters.

Attempts were made to achieve these objectives solely through the use of guide vanes; but all the desired conditions could not be simultaneously achieved, and some other means of establishing the desired flow conditions had to be introduced. The curved entrance annulus used in the previous tests had made difficult the measurement of the inlet mass flow, so that this means was not favored. Kantrowitz, who supervised this design, felt that the use of steady waves emanating from the rotor blades could establish the required flow conditions. Thus, to increase the Mach number at the inner diameters, expansion waves would be produced, and, conversely, compression waves would be generated from the tip sections to reduce the flow velocities relative to the rotor.

For lack of a complete understanding of the three-dimensional character of this steady-wave configuration, the assumption was made that a steady-state flow would exist if a radial summation of the waves across the annulus equalled zero. In the case considered herein, expansion waves of 5° at the root section were assumed to neutralize 5° compression waves produced by the tip section, with no waves at the mean diameter. The rotor-blade entrance conditions were calculated by assuming a steady flow upstream of the rotor (condition 2, fig. 1) unaffected by the waves at the rotor. The entrance region of the rotor blades was then set at an angle to this flow so as to produce waves of the desired strength. The total pressures and total temperatures calculated for condition 2 were presumed to exist after the waves (condition 2').

The stator-entrance conditions at the mean diameter were obtained for a range of guide vane angles from the following assumptions:

- (a) That diffusion to a relative exit Mach number  $\rm\,M_{lj}$  of 0.8 would occur within the rotor at the mean diameter (justified by previous cascade and rotor tests)
- (b) That the relative total pressure loss is equal to that through a normal shock at the entrance Mach number
- (c) A rotor turning angle of  $6^{\circ}$  at the mean diameter to prevent the necessity for large turning angles at the hub diameter

The turning angle at the root and tip sections was then selected to yield uniform exit total pressure across the annulus and to satisfy the conditions for simple radial equilibrium of flow at the exit of the blade.

In practice, these calculations were made with differing assumptions of wave strength, guide-vane turning angles, and entrance axial Mach number until a design satisfying the various requirements mentioned previously was obtained. The flow conditions for this design are presented in figure 1 for air and for Freon-12 gas.

Blade section design. - At the conclusion of tests reported in reference 2, efforts were made to obtain blade sections thicker than those utilized in the shrouded rotor, in order to eliminate the need for a blade shroud. Several two-dimensional blade shapes were obtained graphically and then tested in the cascade equipment described in reference 2. The design method is outlined below:

- (1) A straight surface parallel to the desired entrance flow direction is provided on the rear or lower surface (A to A', fig. 2) to create the "entrance region" (reference 2). Thus, any Mach line originating downstream of A' lies wholly within the blade passage.
- (2) Compression waves are introduced downstream of the entrance region at A' and B' by changing the surface direction at those points. The strength of these compression waves is arbitrarily chosen as one-half that caused by the leading-edge shock at D. The slope of the rear surface remains unchanged between B' and C.
- (3) The leading-edge wedge angle at D must be small enough to permit the flow to remain supersonic downstream of the oblique shock (DE) caused by the wedge and the compressions originating on the rear surface at A' and B'. The supersonic portion of the leading or upper surface is composed of straight-line segments deflected where necessary to cancel the compression waves from A' and B'.
- (4) The width of the throat or minimum distance between blades (EF) is predetermined by the entrance length CD and the average Mach number across CD for which the passage is designed to start. (See reference 6.) The entrance length CD is taken through D and perpendicular to the mean direction of flow since it is assumed that at the instant the passage starts supersonically the normal shock position coincides with CD. The average entrance Mach number is arbitrarily assumed 0.05 less than the weighted average across CD for the calculation of the throat length EF. The position of the throat is determined by the intersection of the shock DE with surface EG drawn parallel to and at the calculated throat distance from BF. A circular-arc fairing tangent to surfaces EG and B'C is then drawn to complete the supersonic portion of the blade section since it is assumed that the normal shock is located along EF.

The passage downstream of the minimum section was constructed to have a very slow rate of diffusion initially followed by a more rapid rate toward the exit. The purpose of the initial slow diffusion was to provide a throat in which the normal shock might be stable at lower Mach numbers than in a rapidly diverging passage. The analysis from which this possibility stemmed is presented in reference 7. The area expansion in the subsonic portion is symmetrical about a circular-arc mean passage line originating halfway between E and F and tangent to required exit

angle at the trailing edge of the rotor. The solidity of the blades is arbitrary, a value close to 3.0 being chosen to obtain reasonable proportions.

## APPARATUS AND METHODS

The compressor test rig (shown schematically in fig. 3) was identical to that described in reference 2, with the exception of the installation of drum-type throttle valve. The throttle consisting of two concentric perforated cylinders, one stationary and the other rotated by an electric actuator, replaced the butterfly vane in an effort to reduce the scale of the turbulence entering the settling chamber. More sensitive throttling control resulted. In addition, the use of remote control allowed one operator to regulate both throttle position and driving turbine speed and resulted in more accurate regulation and longer testing time with the limited supply of compressed air available. The section of the test apparatus upstream of the rotor was altered to create a straight inlet converging about the pitch diameter as shown in figure 4.

Tests were made in Freon-12 gas at or near room temperature and at 0.3 of atmospheric pressure.

Test rotor 1.- Mention was made in reference 2 of a shrouded rotor built to the same aerodynamic specification as the original but more accurately constructed. Greater care was taken in the detail design of the blade tip shroud attachment; a riveted rather than welded joint was used as can be seen in the photograph of the rotor (fig. 5). The construction accuracy was very good.

The rebladed rotor was tested with the expansion ratio found to be optimum in the previous tests  $\left(\frac{Al_4}{A_3} = 1.091, \, \text{fig. 6}\right)$ . Balsa-wood inserts were glued to the inside of the shroud to reduce the annular height at the exit and to provide a smooth surface covering the rivet heads. The contraction ratio of the flow passage  $\left(\frac{A_2}{A_3}, \, \text{fig. 6}\right)$  of 1.086 was obtained by the addition of a balsa-wood fairing on the convex side of each blade. A constant  $10^{\circ}$  wedge of balsa 0.024-inch thick was maintained from root to tip and was faired to zero thickness at the trailing edge, as shown for the pitch section in figure 6. The thickness-chord ratio is identical with that of the Lewis Flight Propulsion Laboratory rotor blades (reference 4); however, the contraction ratio of the airtest rotor is slightly greater because of the increased basic thickness of the blade section.

Preliminary-stage performance tests made with rotor l utilized two rows of untwisted stators to return the flow to an axial direction. Each row consisted of 25 3-inch-chord blades. The leading set was an NACA 65-408 compressor blade section at an angle of 37.4° from the axial direction; the rear set was an NACA 65-(23)08 section at an angle of 11.6° from the axial direction. The stator blade rows were staggered so that the wakes from the upstream blades would pass between the downstream blades.

Test rotor 2.— The unshrouded rotor was designed to have 62 blades and to have a rotor hub width of  $1\frac{3}{4}$  inches. Two-dimensional blade sections were then laid out for each of the three radial stations as previously indicated. The resulting rotor blade sections are presented in table I.

The guide vanes were located upstream of the rotor in a region where the area was 23 percent greater than that immediately ahead of the rotor; therefore, the possibility of exceeding the critical Mach number of the vanes was reduced. The guide-vane design is presented in figure 7.

Details of the rotor construction can be seen in the photograph of the rotor (fig. 8). The blades were machined from 17S-T4 aluminum-alloy stock; the rotor disk, from a 14S-T6 forging. Although the blades are thin (pitch section thickness ratio, approximately 4 percent), no vibrational difficulties were encountered in these tests.

The tip clearance for all tests, 0.015 inch under static conditions, was selected as the minimum clearance permissible. The rotor blades were calculated to stretch 0.005 inch while running at maximum speed in these tests.

Testing procedure.— Compressor test runs were made at preset constant values of rotational speed with no attempt made to hold constant compressor Mach number or equivalent tip speed inasmuch as the rotor speed, Freon purity, and entrance stagnation gas temperature could vary as much as 1 percent, 2 percent, and 10° F, respectively, during a test resulting in a change of equivalent tip speed of as much as 3 percent. Correcting the Freon-test results to corresponding values in air introduced an additional effect upon the equivalent tip-speed parameter and is discussed in the appendix. Since the results of tests in Freon yield qualitative values, these variations in operating conditions were acceptable inasmuch as the desired result – verification or modification of the design assumptions – could be established.

In general, the procedure followed in operating the compressor consisted of first obtaining the desired rotational speed with throttle

open and then gradually increasing the compression ratio noting the throttle position at which surge occurred. The throttle was then opened fully and the process repeated until a throttle position very near the surge point was reached. The flow survey for the maximum-pressure-rise condition was then made. Partially throttled runs were made in a similar manner.

Several tests were made at speeds near design for the maximum-pressure-rise condition since the pressure rise is sensitive to slight variations in throttling.

Instrumentation.— The instrumentation of the compressor installation is completely described in reference 2, but for the sake of continuity of the present paper is briefly reviewed in this section. Fixed static-pressure taps were installed in the settling chamber, in the walls up and downstream of the rotor (see fig. 4), and at the exit of the diffuser. A radial survey of total and static pressure and flow angle made upstream of the rotor indicated that the flow into the rotor was fairly uniform except for a very small boundary layer on each wall. For all operating conditions, radial surveys of total and static pressure and flow direction were taken downstream of the rotor. With the shrouded rotor, the location of the pressure survey was 1.25 inches behind the rotor.

All pressures were recorded simultaneously by photographing a mercury manometer. The rotor speed was measured by a calibrated tachometer.

Total temperature measurements were made in stagnation regions before and after the rotor by means of five thermocouples connected in a series at each station. In addition, calibrated aircraft type of electrical resistance thermometers were installed to supplement the thermocouple readings. All data-reduction methods are based upon temperatures measured by means of thermocouples, since the time lag necessary for the resistance element to come to equilibrium was considerable compared with the length of time available for any test run. However, the temperatures obtained by both means were in good agreement just before shutdown, a result which served as an instrumentation check.

The velocity of sound in the Freon-air mixture was measured by an instrument similar to that described in reference \$. The proportions of the gas constituents and the physical characteristics were then determined.

Reduction of data. The method of performance calculations followed in this paper is fully described in appendix B of reference 2. The weight flow downstream of the rotor was obtained by integration of the elemental weight flow obtained by a radial survey. The upstream flow measurement was based upon wall static and settling-chamber pressure

readings. The inflow and outflow measurements usually agreed within  $2\frac{1}{2}$  percent and were averaged to obtain the values presented.

For the configuration utilizing guide vanes, air was blown at low speed through the compressor test rig with rotor and diffuser removed to obtain the radial distribution of turning angle through the guide vanes.

Two methods of computing the rotor efficiency are available from the data taken: the first, designated  $\eta_t$  is the ratio of the temperature rise for isentropic compression through the weighted total pressure rise to the measured stagnation-temperature rise across the rotor; the second,  $\eta_p$  is the ratio of the useful energy output to the energy input as calculated from momentum and pressure changes. Efficiencies computed by both methods are presented herein because either may be in error by 2 percent at design speed for a temperature-rise-measurement error of  $1^\circ$  F or 2-percent (0.20 inch of mercury) error in exit static-pressure measurement.

## RESULTS AND DISCUSSION

The compressor characteristics of both rotors are presented in terms of equivalent tip speed and weight-flow parameters converted to air flow by the means indicated in the appendix. Although the results have been converted to air for comparison purposes, they are strictly applicable only to these tests made in Freon gas.

# Rotor 1

Rotor alone. The over-all performance of the shrouded rotor without guide vanes is shown in figure 9. At the design tip speed, a pressure ratio across the rotor of 1.98 and an efficiency  $\eta_t$  of 84 percent were measured. Comparison of results reported in reference 2 shows that significant improvement in performance, roughly 10-percent increase in pressure ratio, was obtained by more accurate fabrication of the blades and shroud.

Included in figure 9 are results of a similar rotor tested in air at the Lewis Flight Propulsion Laboratory (reference 4). Although the pressure rise across the compressor measured in air agrees very well with present Freon data, a shift in the surge limit line in the direction of lower flow rates occurred in the air tests. The efficiency of operation in air near design speed is 4 to 5 percent less than that measured in Freon. Machining tolerances and the difference by a factor of 2 in test Reynolds number can explain only small variation in weight flow at

design speed. However, this performance would be explained if the compressor tested in air did not completely attain the supersonic operating condition; that is, the flow in the entrance region of the blade passage was not entirely supersonic. As stated in reference 4, the weight flow is seen to have varied as much as 8 percent with pressure ratio at a tip speed of 1608 feet per second for the air tests; whereas in the Freon tests the flow rate is constant within limits of experimental accuracy. This may in part be attributed to the fact that Freon has a lower starting Mach number for a given contraction than air. Furthermore, Freon, unlike air, will permit an oblique shock to be attached to a 100 wedge at the design Mach number (1.35) for the root section. As mentioned in reference 4, a noticeable pressure-rise field was measured just upstream of the root section; this pressure-rise field indicated the presence of a bow wave. Thus, the flow entering the rotor was apparently not entirely supersonic.

Radial variations of several important factors are shown in figure 10 for the equivalent tip speed of 1610 feet per second in air. The curves have been obtained by averaging results of several tests to eliminate the effects of unavoidable variations of equivalent tip speed. The total pressure ratio across the rotor increases from root to tip, although the rate of increase diminishes toward the tip because the total pressure recovery in the rotor passage falls rapidly in the outer third of the annulus. The rotor tested in air produced a slightly greater total pressure rise in the inner half of the annulus; however, the rapid drop in pressure rise and total pressure recovery in the tip portion of the passage yielded a net weighted average pressure rise approximately equal to that obtained in Freon but at a lower over-all efficiency. The passage pressure recovery in the outer half of the annulus for Freon tests approximates the normal-shock pressure recovery at the relative entrance Mach number (an assumption made in the design of rotor 2). It should be pointed out that the method of computing passage pressure recovery and relative exit Mach number may lead to errors since the total pressure measurement upon which the calculation depends is an average of the main stream and separated region pressure.

A possible explanation of the differences between air and Freon results is that the rotor operating in air had a detached normal shock for a finite portion of its blade length. By the use of Kantrowitz's hypothesis of an upstream wave pattern (reference 1), the stagnation pressure relative to the rotor is reduced an amount approximately equal to the loss through a normal shock at the entrance Mach number. The additional losses through the passage caused by friction and a normal shock occurring at a Mach number close to one after the minimum section are small in comparison. If the outer section of the blade is operating supersonically with an attached oblique shock at the leading edge and with a normal shock after the minimum section, the possibility exists that before the contained shock can be moved far enough forward by

throttling for maximum pressure recovery the increased back pressure will cause stall at the inner diameter and simultaneously a complete stall of the compressor. As evidence that such was the case, the relative exit Mach number near the tip (fig. ll) is shown to have been lower for the air test, yet the passage total pressure recovery was also very much lower. The supposition being advanced is that the Mach number ahead of a normal shock near the rear of the passage at the tip was higher than at the throat section of the tip; therefore, a greater shock loss and severity of the flow separation was created in the case of the air tests. However, separation occurred at the rear of the passage; thereby, the reacceleration of flow usually experienced in a channel behind a normal shock was reduced and lower exit Mach numbers resulted for the air tests. Good agreement between the design rotor turning angles and the measured values was obtained in the Freon tests, as illustrated in figure lo(c).

Rotor in presence of stators. - All tests so far made upon NACA supersonic compressors have been concerned only with the performance of the rotor alone. The possibility existed that the stators might affect the rotor performance because of the pressure fluctuations experienced by the running blades in passing through the pressure field about each stator blade. These pulses might limit the degree to which the compressor could be throttled. Several tests, preliminary in nature, were made with the shrouded rotor (before the addition of the balsa contraction wedge) with the use of two rows of stator blades. Since a cross channel survey after the rotor was not attempted because of interference with the stators, comparison of results, with and without stators, was made on the basis of the total pressure rise measured at the mean diameter and the static-pressure rise measured on the inner and outer casing immediately downstream of the rotor. No discernible differences were noted in the measured quantities; therefore, it was indicated that the operation of the rotor was unaffected by the stators. However, when the blade angle of the front row of stators was increased 50 (decreased angle of attack), the rotor was stalled at all speeds and throttle settings. Apparently reducing the stator angle of attack caused a lower surface stall which in turn reacted on the rotor; the pressure drop through the stators became equivalent to excessive throttling.

Pressure measurements made immediately upstream of the expansion joint (fig. 3) indicated the stator-diffuser combination converted 80 percent of the inlet dynamic pressure to static pressure. The over-all adiabatic efficiency is in doubt because of instrument difficulties. However, if it is assumed that no change in rotor performance occurs because of the stators, the calculated over-all efficiency is 75 percent.

An interesting photograph of the rotor taken after several hours of testing in conjunction with stators is shown in figure 12. Evidence can be seen on the shroud of the position of the shock in the blade passage

and what appears to be separation of flow from the concave surface following the shock. The dark lines are believed caused by the deposition upon impact of suspended oil in the Freon and subsequent adhesion of minute dust particles. Similar streaks were noticed on the shroud after tests with balsa added to one side of the blades. In this instance, the streaks appeared near the minimum sections of the passages.

# Rotor 2

Data were taken to determine the performance of the rotor alone pending the final machining of the guide vanes. The compressor characteristics obtained for rotor 2 when operated without guide vanes are presented in figure 13. Maximum total pressure ratio measured across the rotor varied from 1.29 at 948 feet per second to 2.30 at 1680 feet per second; a value of 2.20 was obtained at equivalent speed of 1610 feet per second and a flow rate of 27.8 pounds per second. The peak adiabatic efficiency of compression at design speed is 84.5 percent.

The guide vanes had a deleterious effect upon the performance of the compressor. At design speed, the total pressure ratio through the unit of 2.03 was less by 8 percent than that measured without guide vanes, although the flow rate remained virtually unchanged (fig. 14). The adiabatic efficiency was reduced 1 percent to a value of 83.5 percent. The rather wide divergence between the  $\eta_t$  and  $\eta_p$  efficiencies for this condition can be traced to differences between the guide-vane turning angles used in the calculation of  $\eta_D$  and the turning that occurred during rotor test runs. The turning angle through the vanes used in calculating  $\,\eta_{_{\mbox{\scriptsize D}}}\,$  was obtained by calibration at low air velocities. The angles were found to be roughly one-half that required. Recent cascade data (reference 9) have disclosed significant reductions in turning angle for a cascade of blades as the Reynolds number is reduced from 350,000, a typical value for the rotor tests, to 100,000, the magnitude of that of the calibration test. Recalculation of one test point with the assumption of design guide-vane turning being realized resulted in better agreement between  $\eta_{\text{D}}$  and  $\eta_{\text{t}}.$  However, the results presented in figure 14(b) for rotor efficiency have not been so corrected.

During operation of the compressor, no discontinuities in performance were noted for either configuration. Operation in and acceleration through the transonic-speed range was accomplished smoothly and represented therefore a stable operating region. The constancy of weight flow at design and higher tip speeds is indicative of supersonic operation with and without guide vanes.

Attempts were made to increase the compressor efficiency at speeds slightly lower than design in a manner suggested by the behavior of supersonic diffusers. The major problem in supersonic diffusers of fixed geometry is one of starting; once the flow into the diffuser is supersonic, theoretically either the contraction ratio may be increased or the entrance Mach number decreased, within limits, without spilling the shock and thereby increasing the diffusion efficiency for a given diffuser. (See reference 5.) Therefore, the possibility was offered of increasing compressor efficiency by reducing the rotational speed after the rotor had attained its design supersonic operating condition and so lowering the entrance Mach number. However, no discernible differences were measured, probably because the pressure disturbances originating downstream of the rotor were sufficiently strong to prevent a stable normal shock in the blade passage at lower Mach numbers. In compressors designed for higher entrance Mach numbers and having greater contraction ratios, this procedure may result in improved performance at lower than design speeds.

The guide vanes do not appreciably affect the radial average total pressure relative to the rotor, and therefore the conclusion could be reached that the pressure ratio across the rotor would be decreased an amount proportional to the loss through the guide vanes. The loss in total pressure of 1 percent calculated for these vanes agrees with that obtained in tests made at the Lewis Flight Propulsion Laboratory on similar vanes (unpublished data) and, therefore, cannot explain the large decrease in pressure ratio when guide vanes are used. With the guide vanes choked at a sufficiently high Mach number, losses in total pressure of 5 percent have been measured. That this is not the case for these tests is evident since the weight flow increased with tip speed for all conditions tested.

Another loss in energy is that caused by the waves propagated upstream. The strength of the waves and the associated loss is considerably less in the absence of the guide vanes. Calculation of the energy dissipated by these waves computed in accordance with reference 1 indicates an efficiency reduction of less than one-half percent and a pressure ratio decrease of 1 percent. The additional mutual interference effects between the guide vanes and rotor are unknown, but small energy dissipations may be produced by the rotor blades in traversing the low velocity wakes of the guide vanes.

The lower pressure ratios obtained with guide vanes would seem to be due more to the difference of rotor inlet conditions caused by the guide vanes and the waves than of losses in the guide vanes and waves.

Radial variations of several performance parameters are shown in figures 15 and 16. When guide vanes are used, the total pressure distribution is fairly uniform and the Mach number of the flow entering

the stators is less than 0.8 at all points; therefore, two of the requirements specified for the rotor have been satisfied. The gas flow has been deflected inward within the rotor as predicted by the design. The turning angle and the flow angle relative to the stators agree with design values in the central portion of the annulus. The turning angle shown is the difference in flow direction relative to the rotor as computed between a plane immediately downstream of the guide vanes and the exit from the rotor and thus includes the wave turning.

The total and static pressure ratios measured across the rotor are lower than those predicted in the design. The noted discrepancy is approximately equal to the difference between estimated and measured total pressure recovery in the passage. However, no account has been taken of the guide-vane losses; the inclusion of these losses would yield better agreement between the design and measured values.

The radial distributions of pressure, velocity, and flow direction, in the absence of guide vanes, are compared in figure 15 with those values estimated by an approximate analysis. A wave condition of equal compression and expansion strengths could not be found. Therefore calculations were made with varying axial Mach numbers until a solution which obeyed the requirements of flow continuity upstream of the waves and at the rotor was found at an inflow axial Mach number of 0.76. The passage turning angles and the relative exit Mach number at the mean diameter were assumed equal to the design values and the rotor performance was then recalculated. Inspection of figure 15 reveals good agreement between recorded and estimated pressure rise and recovery. The flow angle into the rotor upstream of the waves  $\beta_2$  was calculated with the use of the Mach number measured at wall static-pressure taps 1 inch upstream of the rotor where the pressures on the inner and outer inlet surfaces were equal and with the use of the known rotational velocity. The excellent agreement between calculated and estimated angle β2 indicates the validity of the method employed to determine the initial inflow velocity. Except for the tip sections, the pressure recovery in the rotor passage corresponds closely to that estimated. Although diffusion in the rotor passage to lower than estimated Mach numbers was obtained probably because of increased solidity, the total pressure rise is substantially equal to that calculated since the turning through the rotor is less than expected over a major portion of the annulus.

When the guide vanes are used, conditions nearly equal to simple radial equilibrium are established in the rotor passage immediately downstream of the normal shock, the assumption being made as in reference 4 that the design inlet conditions after waves are realized - that is, the position of the normal shock is at the passage throat and the theoretical Mach number after the shock is obtained. Without vanes, the

static-pressure gradient is greater by a factor of three than that necessary for equilibrium. Apparently, the improved diffusion obtained in the absence of the guide vanes refutes the premises advanced in reference 4 regarding the necessity of pressure equilibrium behind the normal shock for maximum diffusion or else the assumptions used therein to calculate the static-pressure gradient behind the shock are invalid. Flow separation behind the normal shock prevents the attainment of the theoretical pressure rise through the shock. That a region of separated flow exists on the rotor blade surfaces because of shock boundary-layer interaction as observed in cascade is indicated by the fact that the average exit Mach number  $\rm M_{\tilde{4}}$  exceeds the value calculated for one-dimensional nonviscous flow. This phenomenon prevents a purely analytical design approach for supersonic compressors and necessitates the use of empirical factors for exit Mach number and total pressure loss.

# SUMMARY OF RESULTS

The results of tests of two NACA axial-flow supersonic compressors are summarized as follows. The 16-inch-tip-diameter rotors were tested in Freon-12 gas and the results were corrected to equivalent values for air.

Thin-blade shrouded rotor. This rotor had a design identical with that of the rotor previously investigated (NACA RM L6J0lb) but was more accurately fabricated. At the equivalent tip speed of 1610 feet per second, a total pressure ratio of 1.98 was obtained which is about 10 percent higher than found in the previous tests. The maximum efficiency of 84 percent and a weight flow of 27.6 pounds per second are slightly greater than the corresponding values of the previous tests.

Comparison with results from a similar rotor tested in air at the Lewis Flight Propulsion Laboratory indicates that somewhat lower weight flow and efficiency were obtained in the air tests, a result attributed to the fact that the flow into the blading in the air tests was not entirely supersonic.

The presence of stators immediately behind the rotor did not affect the rotor performance when the stators were set at their design angle.

Unshrouded rotor. This rotor had thicker blade sections than the shrouded rotor, and guide vanes were incorporated in the design. With guide vanes and at an equivalent tip speed of 1610 feet per second, the unshrouded rotor produced a total pressure ratio of 2.03 with an efficiency of 83.5 percent and weight flow of 28 pounds per second. Operated without guide vanes, the unshrouded rotor produced the corresponding values of 2.20, 84.5 percent, and 27.8 pounds per second, respectively.

The operation of the compressor was smooth and the compressor exhibited no discontinuities in performance through the transonic speed range.

The empirical assumptions used in the design of this type of supersonic compressor, namely, that the relative exit Mach number at the mean diameter is 0.8 and that the total pressure loss is equal to that through a normal shock at the relative entrance Mach number, were found to be in reasonable agreement with the test results.

Langley Aeronautical Laboratory
National Advisory Committee for Aeronautics
Langley Air Force Base, Va.

## APPENDIX

# CONVERSION OF FREON TEST RESULTS TO

# CORRESPONDING VALUES FOR ATR

It is usual to express the performance of compressor elements in terms of the quantity of air handled for a given angular velocity or tip speed. For direct comparison with the numerical values familiar to compressor designers, the results of Freon tests of the supersonic compressor have been converted to the equivalent values in air.

A discussion of the differences which exist in using Freon or air as the testing mediums is presented in appendix D of reference 2. From the example illustrated therein, it is apparent that the inlet Mach number relative to the rotating blade should be made the basis of comparison rather than the compressor Mach number. If it is assumed that design entrance axial Mach number is the same and that no prerotation of the fluid occurs, the relation between rotational speeds in air and Freon may be found as follows:

$$\left(\frac{U}{a_2}\right) = M_2^2 - M_{2a}^2$$

since

$$M_{2_{Air}} = M_{2_{Freon}}$$

$$\left(\mathbf{U}_{\text{Air}}\right)^2 = \left(\frac{\mathbf{a}_{2\text{Air}}}{\mathbf{a}_{2\text{Freon}}}\right)^2 \left(\mathbf{U}_{\text{Freon}}\right)^2 = \frac{\left(\gamma \text{RT}\right)_{\text{Air}}}{\left(\gamma \text{RT}\right)_{\text{Freon}}} \left(\mathbf{U}_{\text{Freon}}\right)^2$$

$$(U_{Air})^2 = \left[\frac{\gamma R}{2 + (\gamma - 1)M_a^2}\right]_{Air} \left[\frac{2 + (\gamma - 1)M_a^2}{\gamma R}\right]_{Freon} (U_{Freon})^2$$

for the same standard stagnation conditions.

In the design utilizing guide vanes, the relation between rotational speeds in air and Freon was determined at the radial station at which there was no turning. The turning and wave strength at the other diameters had to be adjusted to maintain the identical entrance Mach number distribution in the two mediums, as can be seen in figure 2.

The variation of measured inflow axial Mach number from design has a very small effect upon the ratio of rotational speeds, especially if it be assumed that the same discrepancy in Mach number will be noted for air. At speeds lower than design, the equivalent tip speed converted to air is not constant along a characteristic curve since the axial Mach number varies. For these reasons, plus the fact that the purity of Freon varied slightly from test to test, nominal values of equivalent tip speed have been used based upon average inflow Mach numbers and are tabulated as follows:

Free	on	Air			
Tip speed	Rotational speed (rpm)		Rotational speed (rpm)		
768	11,000	1,680	24,020		
733	10,500	1,610	23,020		
698	10,000	1,550	22,180		
663	9,500	1,475	21,100		
628	9,000	1,407	20,120		
524	7 <b>,</b> 500	1,176	16,820		
419	419 6,000		13,560		
384	384 5 <b>,</b> 500		12,380		

To determine the corrected weight flow converted to air, the assumption was made that the axial Mach number at the inlet would be identical in air to that in Freon.

The average inlet Mach number was determined from the following expression:  $\gamma+1$ 

$$\frac{\text{Maximum weight flow}}{\text{Measured weight flow}} = \frac{1}{M_a^2} \left[ \frac{2}{\gamma + 1} \left( 1 + \frac{\gamma - 1}{2} M_a^2 \right) \right]^{\frac{\gamma + 1}{\gamma - 1}}$$

where the maximum weight flow is that flow which would occur for the same stagnation conditions at a Mach number of 1.0.

The equivalent weight for air is then determined from the following expression:

$$W\sqrt{\frac{\theta}{\delta}} = \sqrt{\frac{\gamma}{RT}}pgM_aA$$

where

$$p = 2116\left(1 + \frac{y - 1}{2}M_a^2\right)^{\frac{y}{1-y}}$$

and

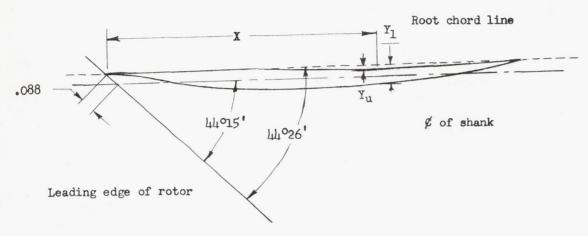
$$T = \frac{518.4}{1 + \frac{\gamma - 1}{2} M_a^2}$$

# REFERENCES

- 1. Kantrowitz, Arthur: The Supersonic Axial-Flow Compressor. NACA Rep. 974, 1950.
- 2. Erwin, John R., Wright, Linwood C., and Kantrowitz, Arthur: Investigation of an Experimental Supersonic Axial-Flow Compressor. NACA RM L6JOlb, 1946.
- 3. Ritter, William K., and Johnsen, Irving A.: Performance of 24-Inch Supersonic Axial-Flow Compressor in Air. I Performance of Compressor Rotor at Design Tip Speed of 1600 Feet per Second. NACA RM E7L10, 1948.
- 4. Johnsen, Irving A., Wright, Linwood C., and Hartmann, Melvin J.:
  Performance of 24-Inch Supersonic Axial-Flow Compressor in Air.
  II Performance of Compressor Rotor at Equivalent Tip Speeds
  from 800 to 1765 Feet per Second. NACA RM E8GO1, 1949.
- 5. Hawthorne, W. R., and Cohen, H.: Pressure Losses and Velocity Changes Due to Heat Release and Mixing in Frictionless, Compressible Flow. Rep. No. E. 3997, British R.A.E., Jan. 1944.
- 6. Kantrowitz, Arthur, and Donaldson, Coleman duP.: Preliminary Investigation of Supersonic Diffusers. NACA ACR L5D20, 1945.
- 7. Kantrowitz, Arthur: The Formation and Stability of Normal Shock Waves in Channel Flows. NACA TN 1225, 1947.
- 8. Huber, Paul W., and Kantrowitz, Arthur: A Device for Measuring Sonic Velocity and Compressor Mach Number. NACA TN 1664, 1948.
- 9. Erwin, John R.: and Emery, James C.: Effect of Tunnel Configuration and Testing Technique on Cascade Performance. NACA TN 2028, 1950.

TABLE I.- ROTOR 2 ORDINATES

(a) Root section (6-inch radius).



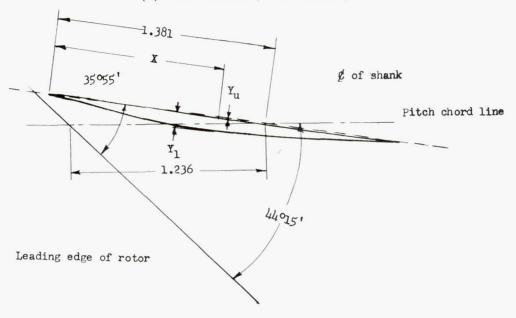
All dimensions in inches

Х	Yu	Yl
0.000 0.072 .100 .135 .148 .200 .300 .349 .390 .400 .500 .600 .700 .714 .800 .900 1.000 1.100 1.200 1.300 1.400 1.500 1.600 1.700 1.800 1.900 2.000 2.100 2.200 2.300 2.100 2.500	0.000 .006 .008 .008 .008 .008 .006 .002 .000002002006010013014016018020023025026028028028028028027026025026027026027026027026009 .000	0.000009013018020028047058067070094114125127130132132132129125121117111103095085075064053041027 .000

NACA

TABLE I.- ROTOR 2 ORDINATES - Continued

(b) Pitch section (7-inch radius).



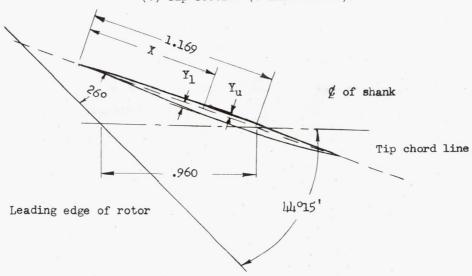
All dimensions in inches

Х	Yu	Yl
0.000 .060 .100 .124 .200 .267 .300 .498 .500 .600 .700 .790 .800 .900 1.000 1.100 1.200 1.300 1.400 1.500 1.500 1.600 1.700 1.800 1.900 2.000 2.158 2.200 2.274	0.000 .005 .008 .009 .008 .008 .007 .006 .006 .006 .005 .003 .003 .003 .002 .001 .000 .000001002003004005008009006004002 .000	0.000005008010017023027037052053069085092092092092092092092089087083078072065059051044036028024015

NACA

TABLE I.- ROTOR 2 ORDINATES - Concluded

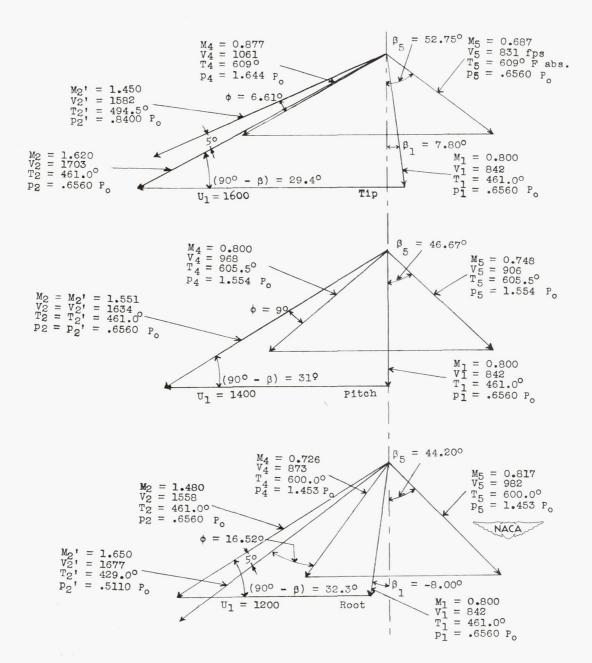
(c) Tip section (8-inch radius).



All dimensions in inches

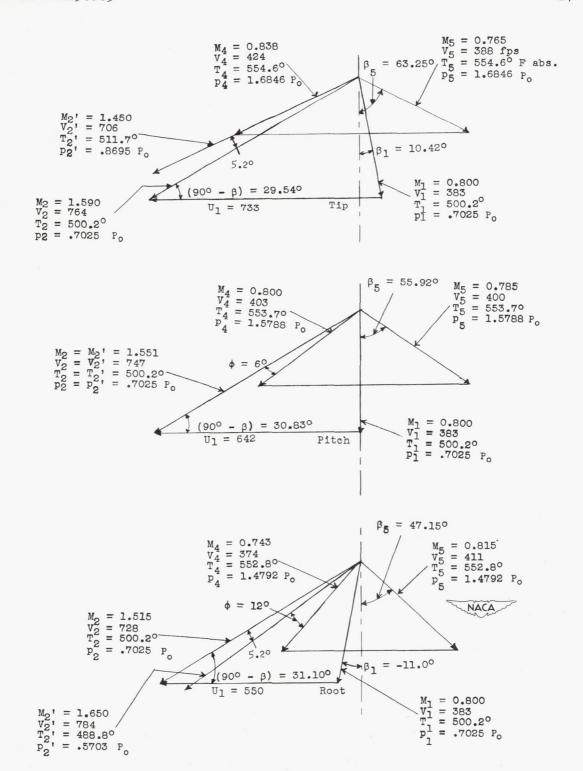
X	Yu	Yl
0.000 .071 .100 .142 .200 .251 .300 .400 .495 .500 .600 .700 .748 .800 .900 .971 1.000 1.100 1.200 1.300 1.400 1.500 1.600 1.700 1.800 1.900 2.000 2.060 2.120	0.000 .007 .009 .011 .012 .014 .015 .018 .020 .022 .023 .023 .024 .023 .023 .023 .023 .023 .023 .023 .020 .018 .016 .013 .010 .005 .003 .002 .001 .0005 .0005	0.000002003004006007008011013014019026031034036035035035032029026023020017015013011010009003 .000

NACA



(a) Velocity diagram for air.

Figure 1.- Supersonic compressor velocity diagrams for the tip, pitch, and root sections.



(b) Velocity diagram for Freon corresponding to the air design as shown in figure 1(a).

Figure 1. - Concluded.

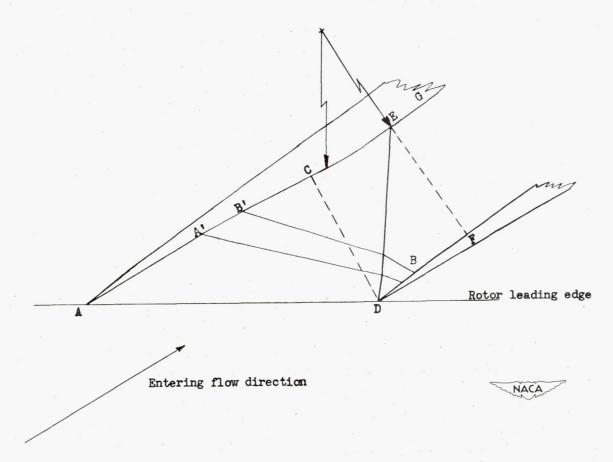


Figure 2.- Supersonic region of a two-dimensional rotor blade section.

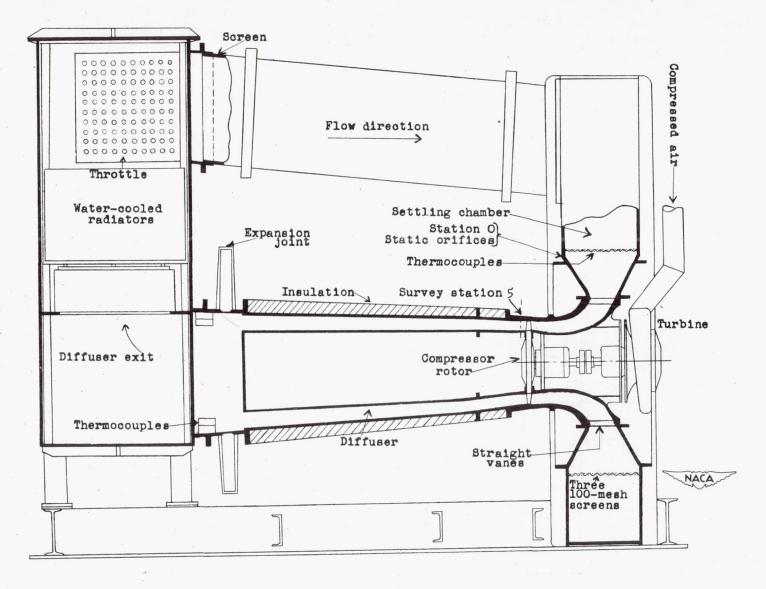


Figure 3.- Sectional view of the supersonic-compressor test setup.

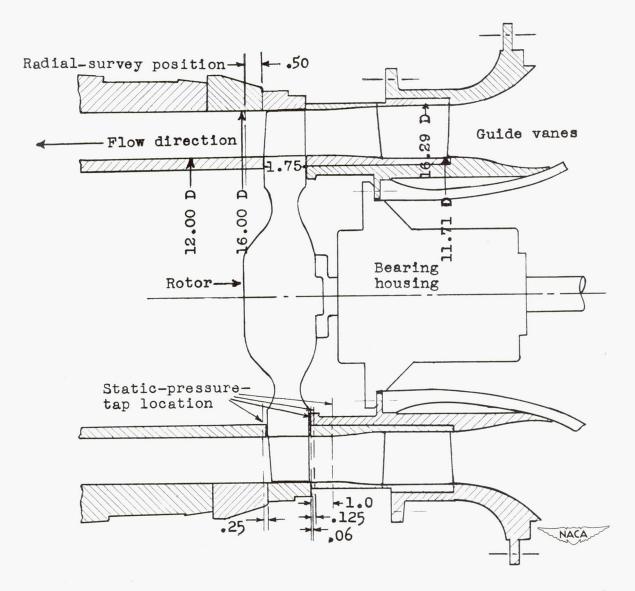


Figure 4.- Arrangement of rotor, guide vanes, and inlet passages and location of pressure instrumentation. All dimensions are in inches.

31

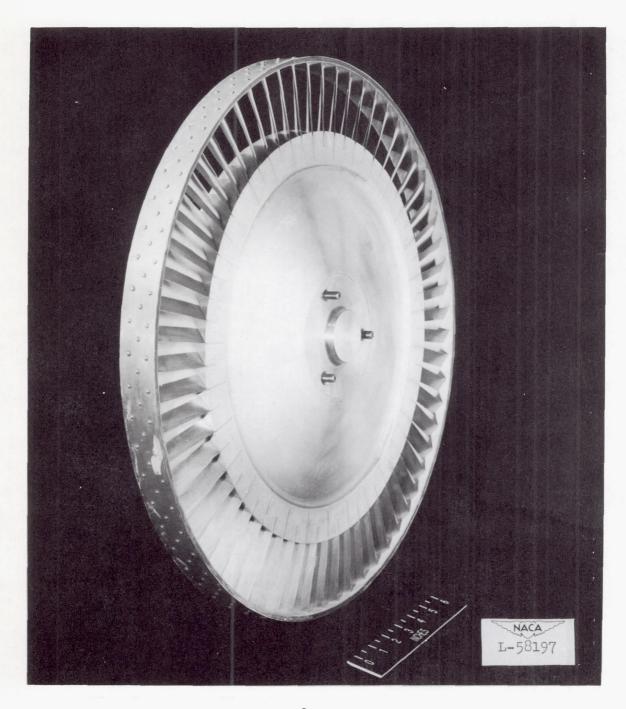


Figure 5.- Rotor 1 with 10° wedge of balsa on the blades.

					-
					,

2

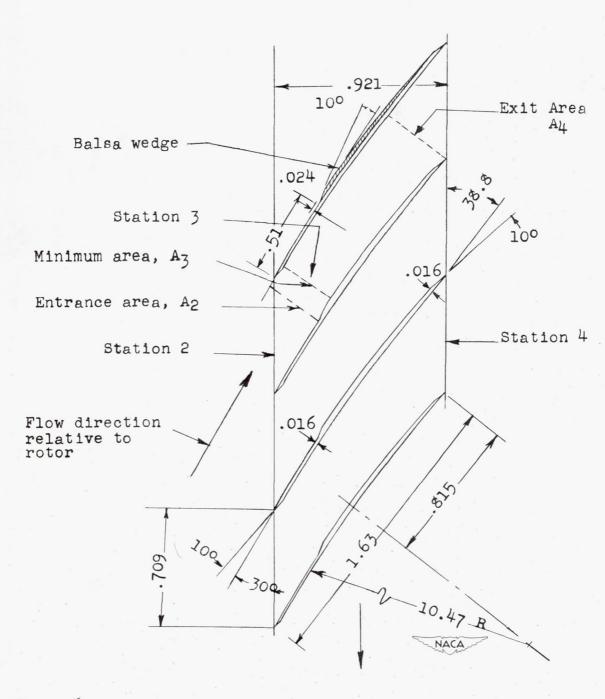


Figure 6.- Cross section through rotor 1 blades at 14-inch (pitch) diameter. Design configuration; 62 blades used. (All dimensions are in inches.)

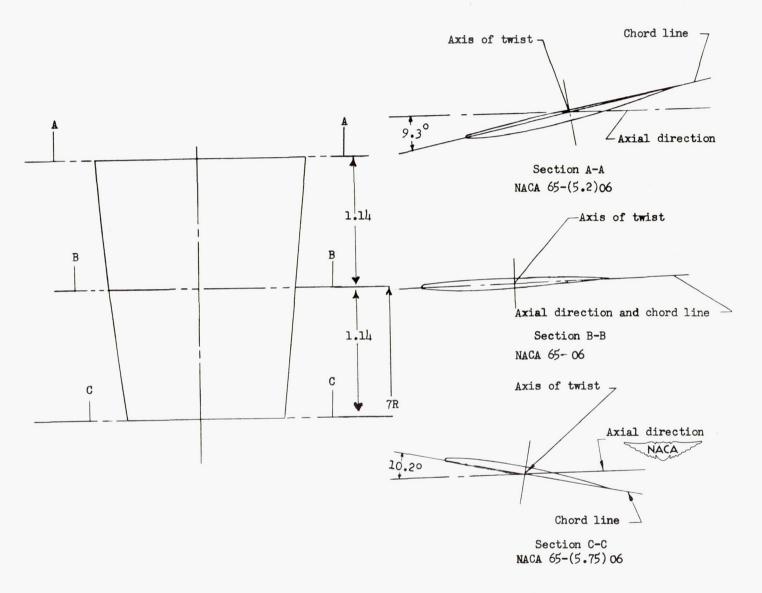


Figure 7.- Guide-vane design for rotor 2.

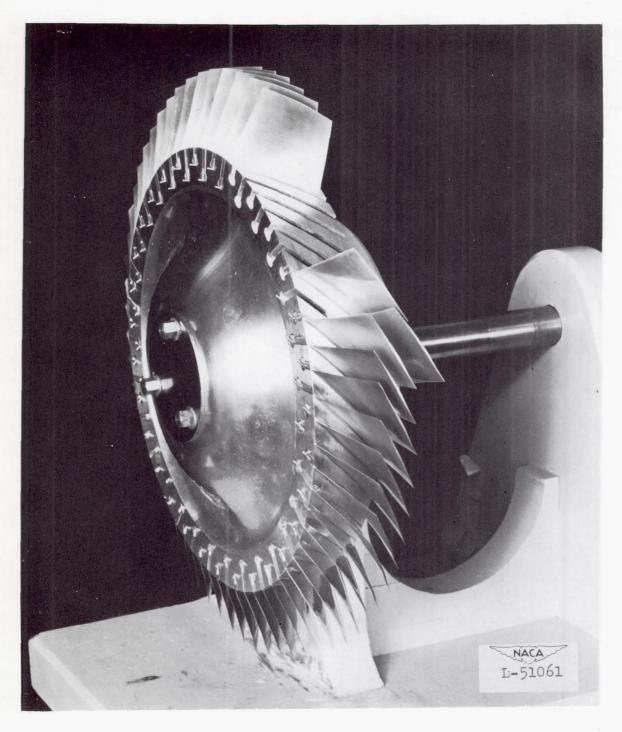
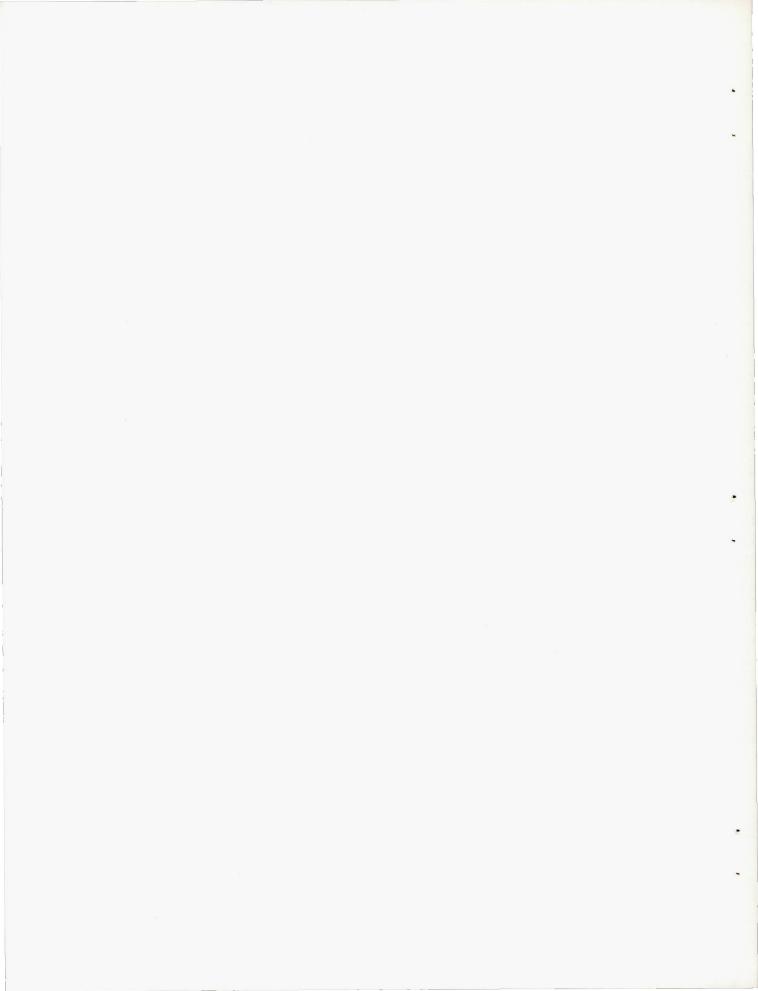
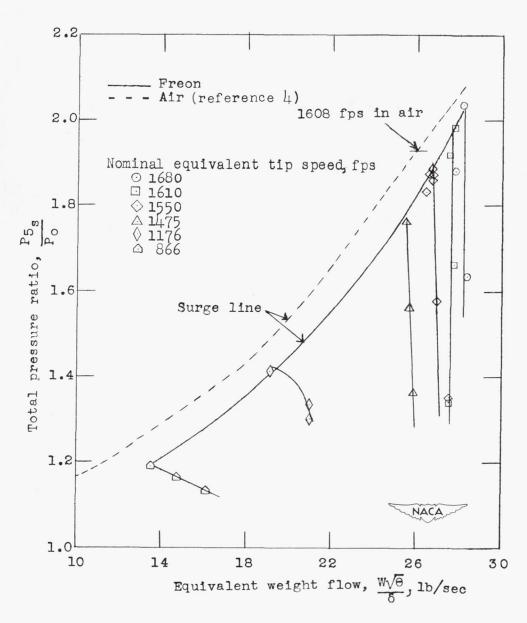


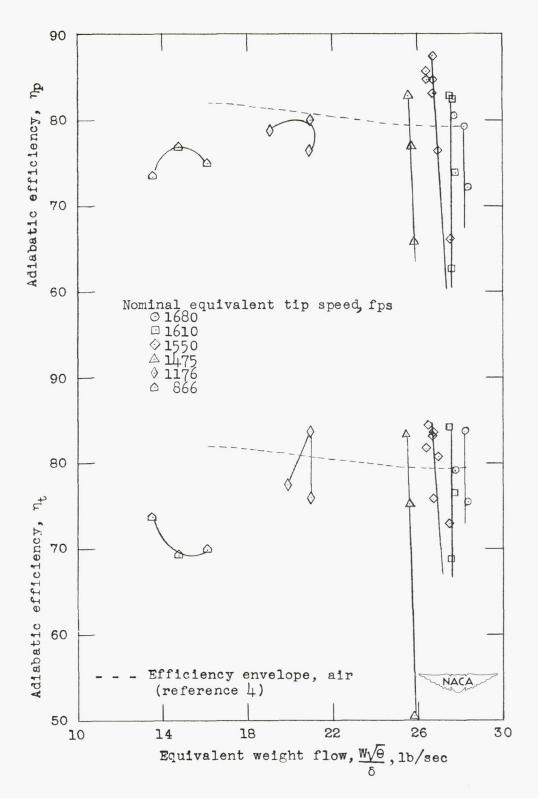
Figure 8.- Rotor 2 before final assembly.



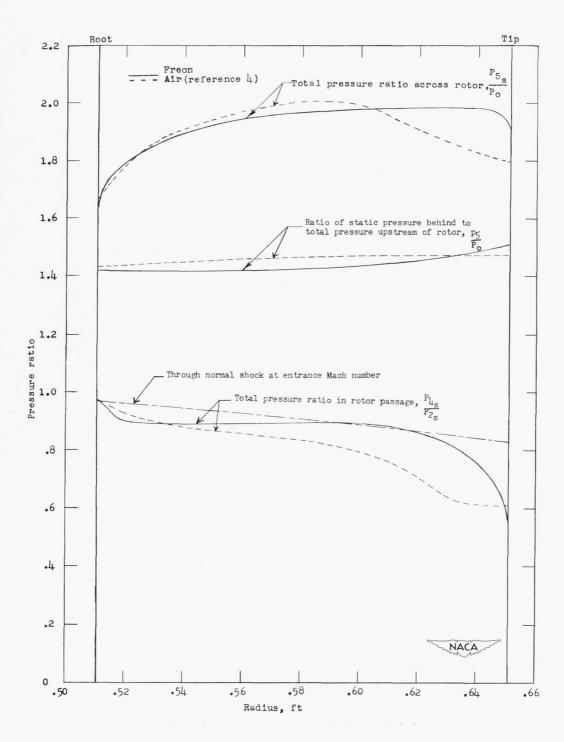


(a) Total pressure rise.

Figure 9.- Characteristics of rotor 1. Results corrected to air flow.

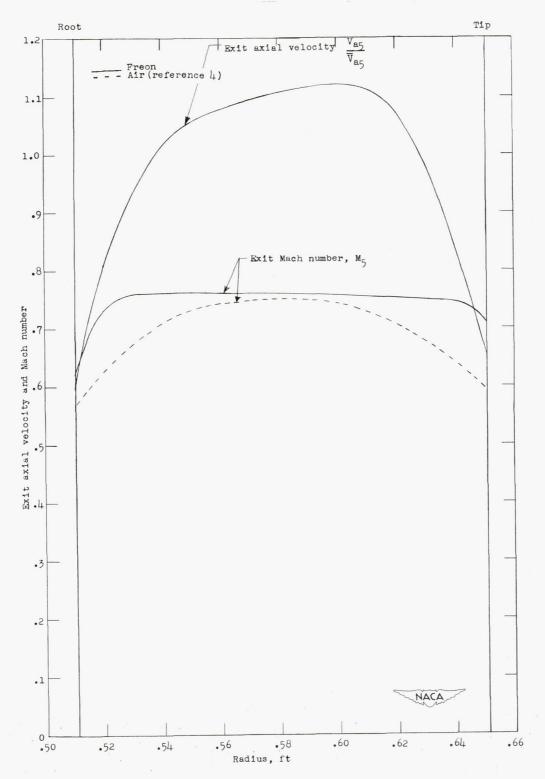


(b) Efficiency.



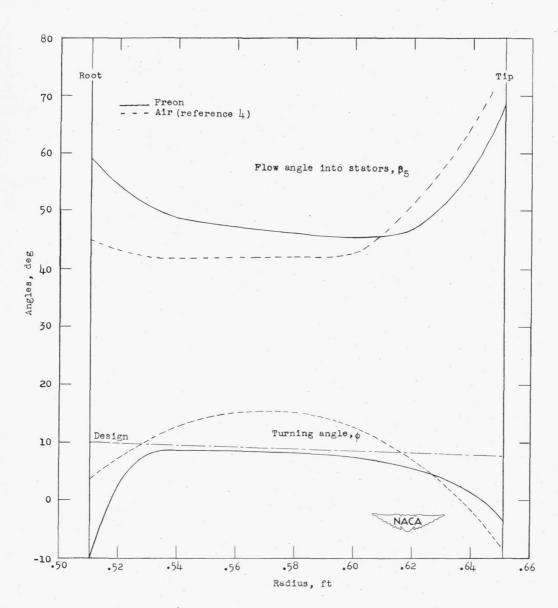
(a) Pressure ratios.

Figure 10.- Radial variation of compressor parameters at design equivalent tip speed for rotor 1.



(b) Exit axial velocity ratio and Mach number.

Figure 10. - Continued.



(c) Absolute exit and turning angles.

Figure 10.- Concluded.

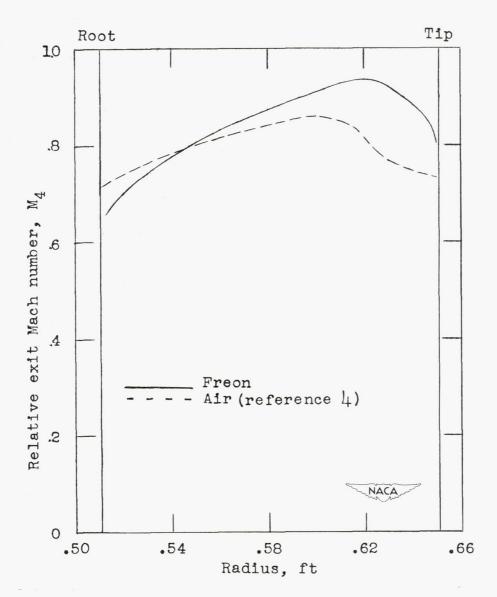


Figure 11.- Comparison of the relative Mach number at the exit of rotor passage at design equivalent tip speed.

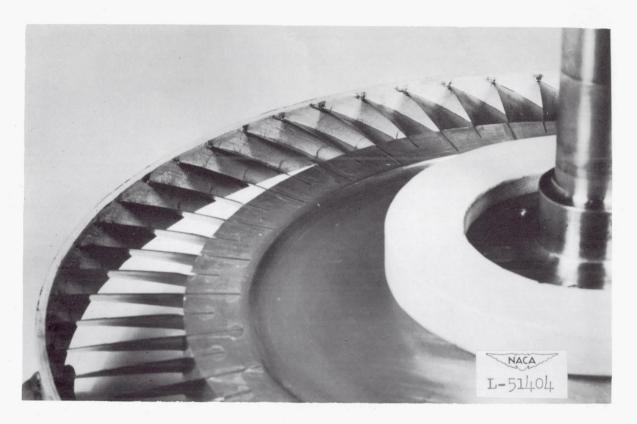
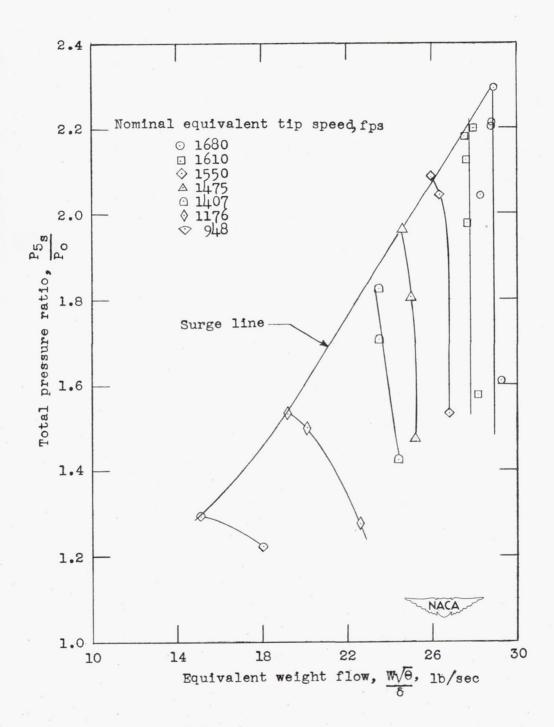
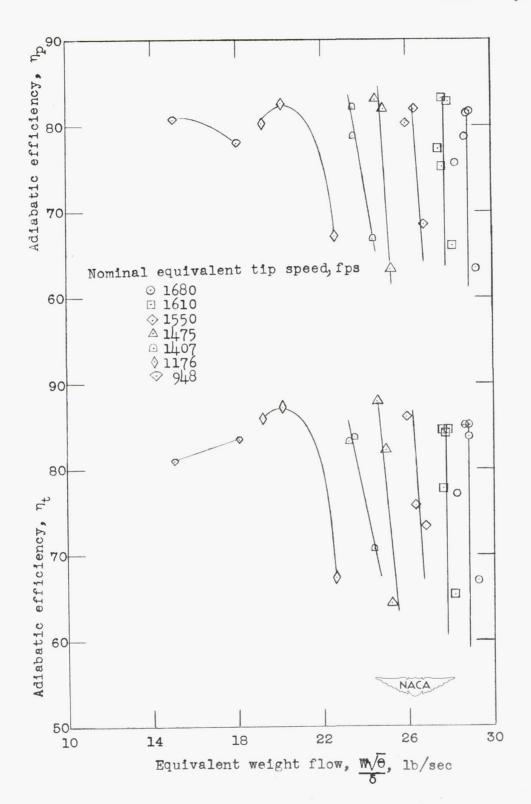


Figure 12.- View of rotor 1 without balsa showing dust deposition on outer shroud.



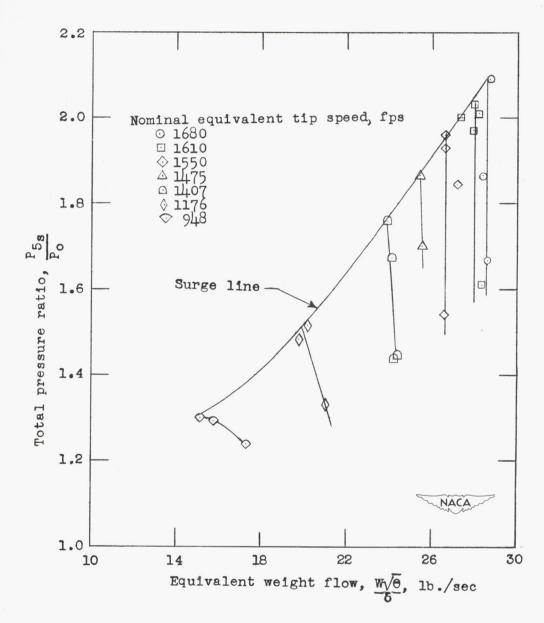
(a) Total pressure rise.

Figure 13.- Characteristics of rotor 2 without guide vanes. Results corrected to air flow.



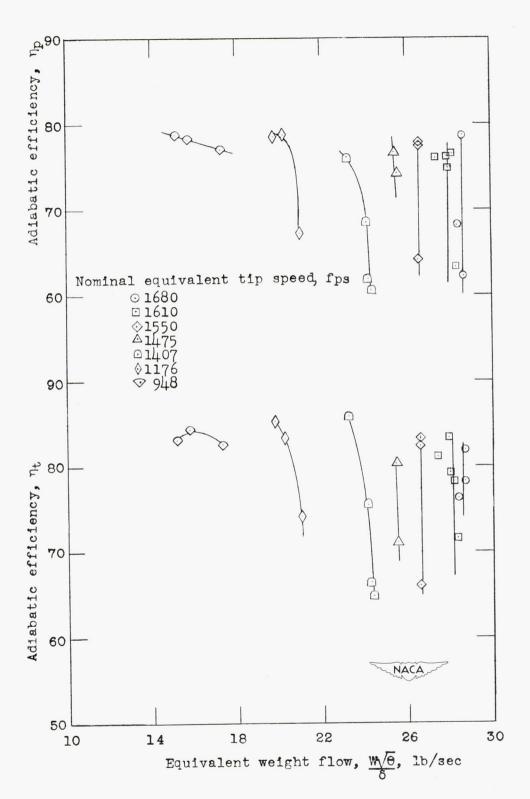
(b) Efficiency.

Figure 13.- Concluded.



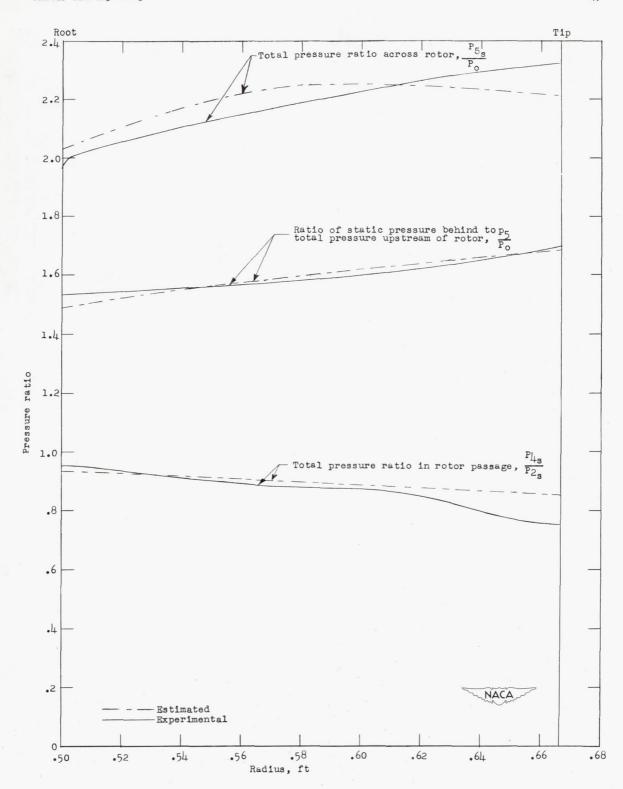
(a) Total pressure rise.

Figure 14.- Characteristics of rotor 2 with guide vanes. Results corrected to air flow.



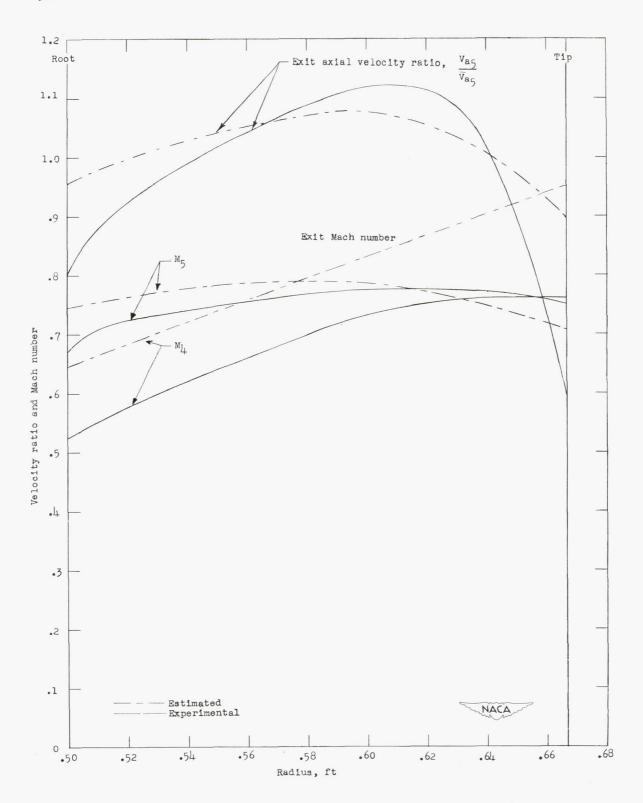
(b) Efficiency.

Figure 14. - Concluded.



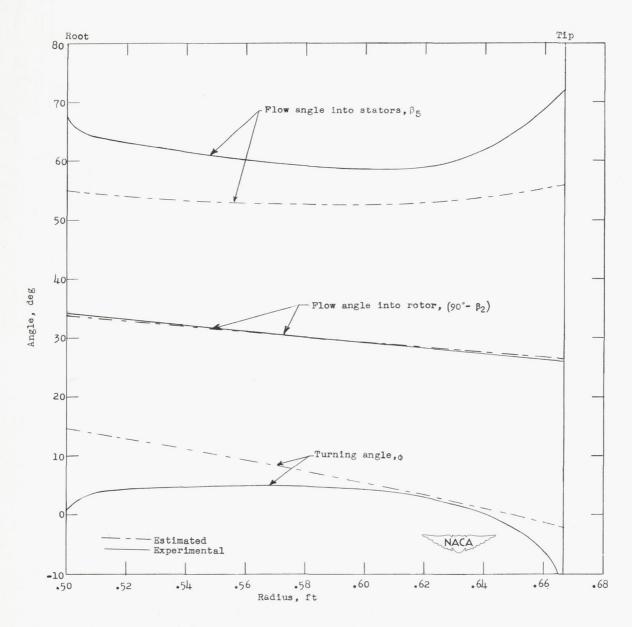
(a) Pressure ratios.

Figure 15.- Radial variation of compressor parameters at an equivalent tip speed of 1610 feet per second for Freon rotor 2 without guide vanes.



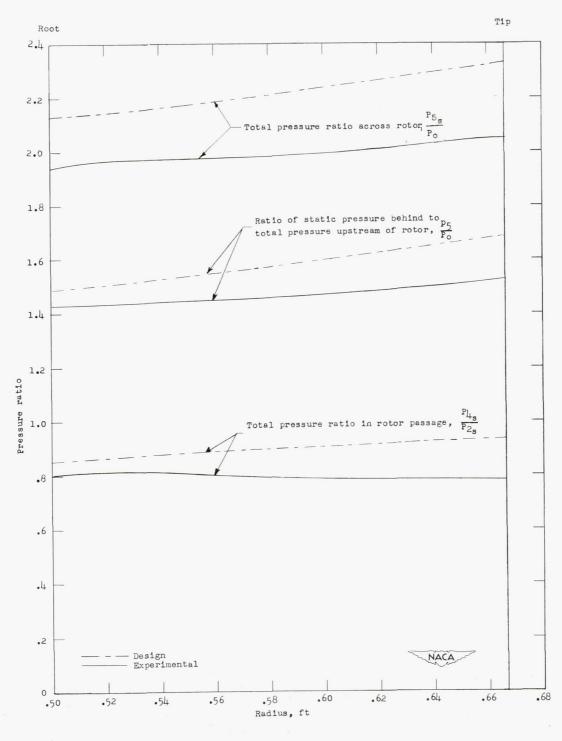
(b) Exit axial velocity ratio and Mach number.

Figure 15. - Continued.



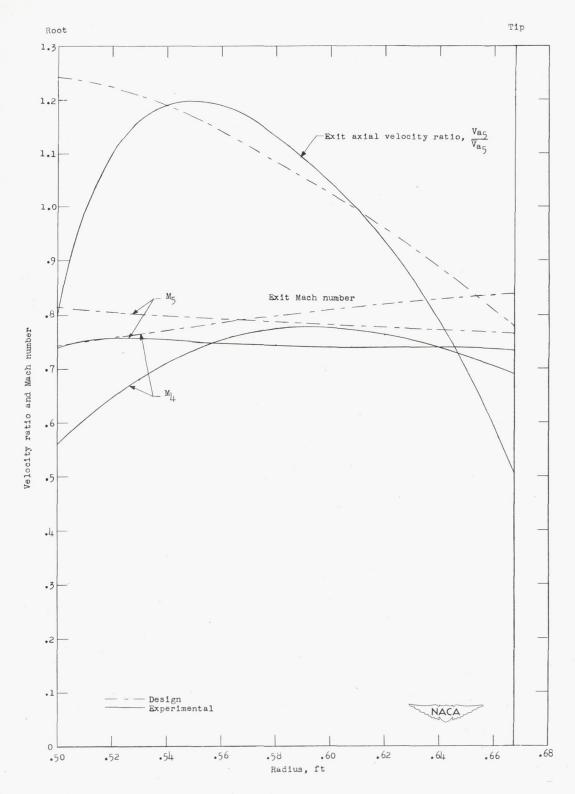
(c) Absolute exit and turning angles.

Figure 15.- Concluded.



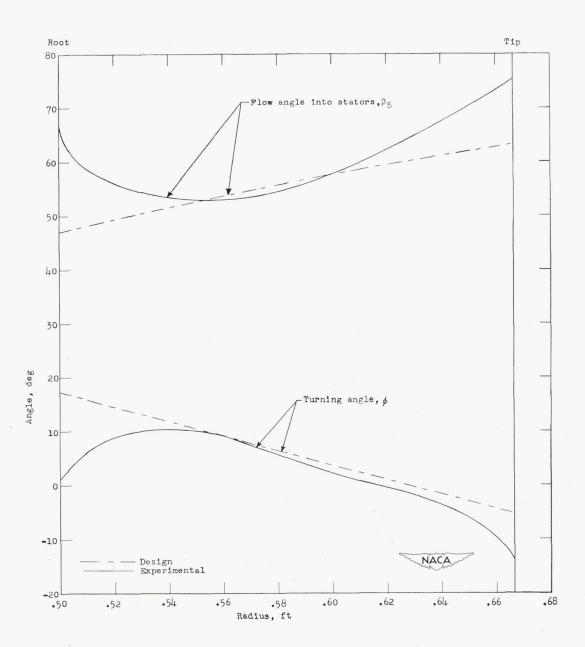
(a) Pressure ratios.

Figure 16.- Radial variation of compressor parameters at an equivalent tip speed of 1610 feet per second for Freon rotor 2 with guide vanes.



(b) Exit axial velocity ratio and Mach number.

Figure 16.- Continued.



(c) Absolute exit and turning angles.

Figure 16.- Concluded.